

Permanent Electric Dipole Moment of Cerium Monoxide[†]

Colan Linton,^{*,‡} Jinhai Chen,[§] and Timothy C. Steimle[§]

Centre for Laser Atomic and Molecular Sciences and Physics Department, University of New Brunswick, P.O. Box 4400, Fredericton, New Brunswick E3B 5A3, Canada, and Department of Chemistry and Biochemistry, Arizona State University, Tempe, Arizona, 85287-1604

Received: February 5, 2009; Revised Manuscript Received: March 17, 2009

Stark spectra of the [16.5]2-X₁2 and [16.5]2-X₂3 transitions of cerium monoxide (CeO) have been obtained at a resolution of ~50 MHz. Analysis of the Stark spectra yielded permanent electric dipole moments, μ_{el} , of 3.119(8), 3.115(7), and 2.119(8) D for the X₁2, X₂3, and [16.5]2 states, respectively. The ground X₁2 state dipole moment is shown to follow the trend shown by other lanthanide oxides. While most ab initio calculations tend to overestimate the ground state dipole moment, the value calculated by using pseudopotentials in which the 4f orbital participates in the chemical bonding (Dolg,M.; Stoll, H.; Preuss, H. *THEOCHEM* 1991, 231, 243] is in very good agreement with our experimental value.

Introduction

The permanent electric dipole moment, μ_{el} , is a very valuable tool in our attempts to gain insight into the electronic structure of diatomic molecules and to assess the quality of a variety of methodologies for electronic structure calculation. For most of the lanthanide oxides, the low-lying electronic states are derived from the 4f^Nσ(6s6p) configuration of the metal ion (M²⁺) core.^{1–3} The σ orbital is strongly polarized away from the oxygen (O²⁻) ligand, moving the center of negative charge closer to the positive core and reducing μ_{el} . Experimentally determined values of μ_{el} are therefore useful indicators of the degree of this back polarization. We have been conducting a systematic examination of the trend in the value of μ_{el} for the oxides across the lanthanide group and have recently measured μ_{el} for HoO⁴ and NdO⁵ to add to earlier measurements for YbO,⁶ SmO,⁷ DyO,⁸ and LaO.⁹ We also measured the dipole moment of UO,¹⁰ whose ground state configuration is identical with that of NdO (i.e., U²⁺(5f³7s)O²⁻ vs. Nd²⁺(4f³6s)O²⁻) and found that the dipole moments of the two molecules are nearly identical. A plot (Figure 4 in ref 10) of all the experimental μ_{el} values for the ground states of the lanthanide oxides shows a smooth trend, represented by an empirical curve that is a second order polynomial fit to all the measured μ_{el} values. While there is an obvious increase in μ_{el} toward the heavier lanthanides, it is not obvious whether the curve flattens out at the low mass end or exhibits a minimum. To resolve this, we need to fill in the gap between NdO and LaO by measuring μ_{el} for CeO and PrO. In this paper, we describe our measurement of μ_{el} for CeO from the analysis of the optical Stark effect.

The field free spectrum of CeO has been well studied at Doppler limited resolution. Barrow et al.¹¹ obtained photographic spectra and rotationally analyzed about 40 transitions. Linton et al.¹² used laser induced fluorescence to provide energy linkages for seven low-lying states and, in a subsequent publication, Linton et al.¹ combined all the laser induced fluorescence and photographic spectra to provide further energy

linkages for the low-lying states and to correlate them with the lower states of transitions observed in the photographic spectra. A ligand field theory (LFT) approach was introduced to describe the low-lying states^{1,13} and all 16 electronic states expected from the ground state configuration {Ce²⁺(4f6s)O²⁻} were identified and a global electronic energy level pattern was established. Many of the low-lying states were observed only through dispersed fluorescence at low resolution and their energies were thus determined only to within ±3 cm⁻¹. Kaledin et al.¹⁴ in an extensive investigation using laser excitation spectroscopy observed many transitions at high resolution and determined accurate term energies and rotational constants for all 16 low-lying states.

LFT has been successful in predicting the order and energies of the low-lying states of lanthanide-containing molecules.^{1–3,14} These molecules are in the Hund's case c coupling limit and are characterized by the projection of the electronic angular momentum along the internuclear axis Ω and the total angular momentum J. LFT establishes the approximate relationship between Ω and J and the atomic angular momentum for M²⁺. The Russell–Saunders term for the ground state of the 4f electron core is ²F_{2,5} and the total angular momentum quantum number is J_c = 2.5. This combines with the 6s electron to give two states with total atomic angular momentum J_a = 2 and 3. The projection of J_a on the internuclear axis then gives Ω. Of particular interest for the present study are the two lowest lying states, X₁2(J_a=2,Ω=2) and X₂3(J_a=3,Ω=3). The separation of the lowest rotational levels of these two states, X₁2(J=2) and X₂3(J=3) was found to be only 84.452 cm⁻¹.¹⁴ The two states differ only in the orientation of the angular momenta of the 4f electron core and the 6s electron, which has little bearing on the overall energy because of the spatial disparity of the 6s and 4f electrons. We describe below our measurement of the dipole moments for these two states to see if the ground state dipole moment follows the trend shown by the other lanthanide oxides and if the relative orientation of the 4f and 6s electron angular momenta affects the dipole moment.

Experimental Section

The supersonic molecular beam apparatus and laser induced fluorescence (LIF) optical detection scheme for the Stark

[†] Part of the "Robert W. Field Festschrift".

^{*} To whom correspondence should be addressed. Phone: (506)453-4723. Fax: (506)453-4581. E mail: colinton@unb.ca.

[‡] University of New Brunswick.

[§] Arizona State University.

TABLE 1: Wavenumbers and Constants (cm⁻¹) for the [16.5]2-X₁2 and [16.5]2-X₂3 Transitions of CeO

| Wavenumbers | | | | | | |
|-------------|------------------------------|-----------------------|-----------------------|------------------------------|-----------------------|-----------------------|
| <i>J</i> | [16.5]2-X ₁ 2 0-0 | | | [16.5]2-X ₂ 3 0-0 | | |
| | <i>R</i> (<i>J</i>) | <i>Q</i> (<i>J</i>) | <i>P</i> (<i>J</i>) | <i>R</i> (<i>J</i>) | <i>Q</i> (<i>J</i>) | <i>P</i> (<i>J</i>) |
| 2 | 16526.2056 | 16524.1433 | | | | |
| 3 | 16526.8297 | 16524.0802 | 16522.0223 | 16444.5036 | 16441.7493 | 16439.6854 |
| 4 | 16527.4318 | 16523.9942 | 16521.2453 | 16445.0859 | 16441.6452 | 16438.8954 |
| 5 | 16528.0165 | 16523.8882 | 16520.4444 | 16445.6411 | 16441.5164 | 06438.0774 |
| 6 | 16528.5756 | 16523.7592 | 16519.6365 | 16446.1713 | 16441.3583 | 16437.2324 |
| 7 | | 16523.6111 | 16518.8014 | 16446.6762 | 16441.1742 | 16436.3603 |

| Constants | | | | | | |
|-----------|------------------|--------------|------------------|--------------|---------------|--------------|
| <i>T</i> | X ₁ 2 | | X ₂ 3 | | [16.5]2 | |
| | <i>T</i> | <i>B</i> | <i>T</i> | <i>B</i> | <i>T</i> | <i>B</i> |
| 0 | | 0.354465(49) | 84.0940(13) | 0.356932(54) | 16524.1649(9) | 0.343839(42) |

| Correlation Matrix ^a | | | | | |
|---------------------------------|---------------------|---------------------|---------------------|------------|------------|
| | B{X ₁ 2} | T{X ₂ 3} | B{X ₂ 3} | T{[16.2]2} | B{[16.2]2} |
| B{X ₁ 2} | 1.00 | | | | |
| T{X ₂ 3} | 0.44 | 1.00 | | | |
| B{X ₂ 3} | 0.59 | 0.30 | 1.00 | | |
| T{[16.2]2} | 0.42 | 0.67 | 0.11 | 1.00 | |
| B{[16.2]2} | 0.76 | 0.08 | 0.78 | 0.14 | 1.00 |

^a Standard deviation of fit = 0.0020 cm⁻¹.

measurements were the same as those used for our recent experiments on UO¹⁰ and NdO⁵ with a cerium rod replacing the uranium and neodymium rods of the previous experiments. Two transitions, [16.5]2-X₁2 and [16.5]2-X₂3 were chosen for investigation (the upper states are labeled [10⁻³T₀(cm⁻¹)]Ω) and were probed with the output of a single frequency ring dye laser with Rhodamine 6G in the 605–609 nm region. Spectral line widths of ~50 MHz full width half-maximum were achieved by the combination of molecular beam collimation and low laser intensity. The resulting LIF was detected through a ±10 nm bandpass filter centered at 620 nm and processed by using gated photon counting.

For the Stark measurements, static electric fields of up to 1250 V/cm were generated by application of a voltage across a pair of highly transmitting, conducting neutral density filters placed across the region of molecular fluorescence. The field strength was calibrated by using a voltmeter and mechanical measurement of the Stark plate spacing. The systematic uncertainties in the electric field strength calibration were estimated to lead to a maximum of 2% uncertainty in the spectral shift measurements.

A polarization rotator and polarizing filter were used to orient the electric field vector of the linearly polarized laser radiation either parallel or perpendicular to the applied electric field. This allowed us to isolate transitions that obeyed the Δ*M_J* = 0 (parallel) or ±1 (perpendicular) selection rules, where *M_J* is the projection of *J* (the total angular momentum) along the field direction. Relative frequency calibration of the laser output was established by diverting a fraction of the beam through a pressure and temperature stabilized 10 cm confocal etalon [free spectral range (fsr) = 749.14 MHz]. A second, unstabilized, 1 m confocal etalon (fsr = 75 MHz) was used to interpolate between transmission peaks of the 10 cm confocal etalon. The absolute wavenumbers were determined to an accuracy of ±0.0001 cm⁻¹ by simultaneously recording the sub-Doppler I₂ absorption spectrum.^{15,16} Lines of the I₂ B-X transition were recorded at sub-Doppler resolution to provide precise absolute frequency markers.

Results

Field Free Spectra. Of the two transitions investigated, the [16.5]2-X₁2 transition had been observed photographically and analyzed¹¹ and the [16.5]2-X₂3 transition was being observed for the first time. As our resolution was an order of magnitude better than the previous observation, we took field free spectra of the low *J* lines in both transitions and performed a rotational analysis, fitting the term energies of each state to the simple formula

$$T = T_0 + B[J(J + 1) - \Omega^2] \quad (1)$$

As data were taken only up to *J* = 7, the centrifugal distortion term, *D*, was not required. The data and the final parameters are presented in Table 1. Our value of *T*₀ = 84.0940 cm⁻¹ for the X₂3 state differs from the value of 82.30 cm⁻¹ quoted by Kaledin et al.,¹⁴ who fitted their data to *BJ*(*J* + 1) rather than *B*[*J*(*J* + 1) - Ω²], which is appropriate for a case c molecule. A fit of our data to *BJ*(*J* + 1) gives *T*₀ = 82.2995 cm⁻¹. We find a separation of 84.4571(8) cm⁻¹ between the lowest rotational levels, X₂3(*J*=3) and X₁2(*J*=2), in excellent agreement with Kaledin et al.

Stark Effect. Stark spectra were taken of the first two lines in each branch, i.e., *R*(2), *R*(3), *Q*(2), *Q*(3), *P*(3), and *P*(4) of the [16.5]2-X₁2 transition and of the first lines *R*(3), *Q*(3), and *P*(3) of the [16.5]2-X₂3 transition. Spectra were obtained at several different electric field strengths and with the laser polarized both parallel and perpendicular to the electric field in order to isolate the Δ*M_J* = 0 and Δ*M_J* = ±1 transitions. The Stark splittings were clearly resolved and, for both transitions, varied linearly with the electric field strengths. Figures 1 and 2 show observed and calculated Stark spectra of the two transitions.

There was no evidence of Ω doubling in either transition. Therefore, at the low applied electric fields used in these experiments, the Stark shifts are well described by the degenerate perturbation theory expression for the Stark operator ($\hat{H}^{\text{Stark}} \equiv -\vec{\mu}_{el} \cdot \vec{E}$):

$$\Delta v_{\text{Stark}} = \langle \Psi^{\text{elc.}}; J\Omega M_J \pm | \hat{H}^{\text{Stark}} | \Psi^{\text{elc.}}; J\Omega M_J \mp \rangle = \frac{-\mu_{\text{el}} E M_J \Omega}{J(J+1)} (0.5034 \text{ MHz/D}) \quad (2)$$

In eq 2 Δv_{Stark} is in MHz, μ_{el} is in Debye, E is in volt/cm, and the numerical factor of 0.5034 converts from SI to experimentally measured units.

A total of 207 [16.5]2–X₁2 and 89 [16.5]2–X₂3 transitions were measured and all the Stark shifts for both transitions (listed in Tables 1 and 2 in the Supporting Information) were included in a single global least-squares fit. The resulting dipole moments for the three states, associated uncertainties, and correlation coefficients are presented in Table 2. The standard deviation of the fit was 9 MHz, which is commensurate with the measurement uncertainty. The spectra calculated by using the dipole moments in Table 2 are shown in Figures 1 and 2 to reproduce the observed spectra very well.

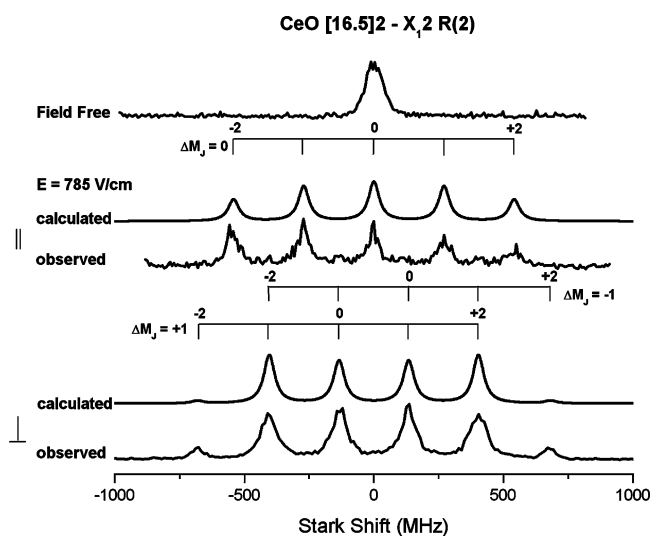


Figure 1. The $R(2)$ line of the 0–0 band of the [16.5]2–X₁2 transition of CeO recorded field free (top) and at a field strength of 785 V/cm with the laser polarized parallel (middle) and perpendicular (bottom) to the electric field. Calculated spectra are shown above the observed spectra and the lines are labeled with their lower state M_J value.

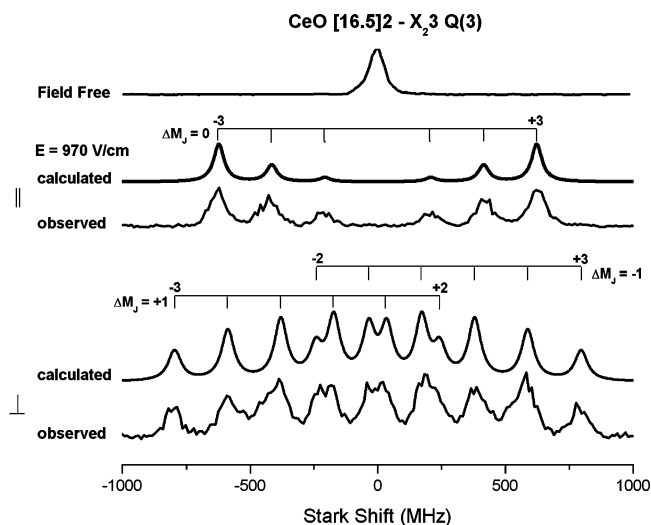


Figure 2. The $Q(3)$ line of the 0–0 band of the [16.5]2–X₂3 transition of CeO recorded field free (top) and at a field strength of 970 V/cm with the laser polarized parallel (middle) and perpendicular (bottom) to the electric field. Calculated spectra are shown above the observed spectra and the lines are labeled with their lower state M_J value.

TABLE 2: Permanent Electric Dipole Moments of CeO

| state | exptl ^a | theory |
|------------------|--------------------|---|
| X ₁ 2 | 3.119(8) D | 3.80, ^b 3.873, ^c 3.071, ^d and 4.417 ^e |
| X ₂ 3 | 3.115(7) D | |
| [16.5]2 | 2.119(8) D | |

^a Correlation coefficients: X₁2/X₂3 = 0.40, X₁2/[16.5]2 = 0.74, X₂3/[16.5]2 = 0.54. Standard deviation of fit = 8.9 MHz. Numbers in parentheses represent 2 σ standard error estimates. ^b Reference 17. ^c Reference 18 with 4f orbitals in the pseudopotential core. ^d Reference 18 with 4f orbitals in the valence space. ^e Reference 19.

The uncertainties quoted for the dipole moments in Table 2 represent the 2 σ standard deviations from the least-squares fit and attest to the high quality of the data. They do not account for possible systematic errors in measurement of the Stark plate separation and the electric field. A conservative maximum uncertainty of 2% in these measurements would give maximum possible uncertainties of ~ 0.06 D for the two lower states and ~ 0.04 D for the upper state.

Discussion

The dipole moments of the ground X₁2 and the X₂3 states, 3.119 and 3.115 D, are almost identical, which shows that the electron charge distribution is not affected by the relative orientation of the angular momenta of the 4f and 6s orbitals. The value of μ_{el} is close to the value of 3.18 D predicted from the empirical quadratic curve in ref 10. The increase in dipole moment with increasing atomic number across the lanthanide oxide group has been discussed in detail in previous papers^{5,10} and is caused by the imperfect screening of each added f electron reducing the amount of back polarization of the σ orbital thus increasing the dipole moment. There appears to be a slight decrease in the value of μ_{el} from 3.207 to 3.119 D in going from LaO to CeO, i.e., from the metal centered 6s to 4f6s configuration. A more meaningful measure of the charge distribution is obtained from the value of μ_{el}/R_c which effectively indicates the effective charge on the atoms. For CeO the effective charge is 0.357e, just slightly lower than that of LaO (0.365e).

There have been several theoretical calculations of the dipole moments of the lanthanide oxides. Dolg and Stoll¹⁷ calculated the spectroscopic properties for the entire Lanthanide oxide series using energy adjusted pseudopotentials in a SCF/CI calculation and found $\mu_{\text{el}} = 3.80$ D for CeO and a bond length of 1.974 Å, compared to the experimental value of 1.820 Å. This leads to an effective charge of 0.40e. In a later paper concentrating entirely on the properties of the 16 low-lying states of CeO arising from the 4f σ configuration, Dolg et al.¹⁸ performed energy adjusted CISD calculations within the ΛS coupling scheme “with the quasirelativistic pseudopotential for Ce including the 4f orbitals in the valence space”, i.e., with the 4f electrons making a significant contribution to the bonding. For the ³ Φ ground state, they found $\mu_{\text{el}} = 3.071$ D and $R_c = 1.827$ Å in excellent agreement with the experimental values. The average values over all states in the 4f σ superconfiguration were $\mu_{\text{el}} = 3.093$ D and $R_c = 1.821$ Å. They also performed calculations in which, as in previous calculations,¹⁷ the 4f orbitals are attributed to the pseudopotential core, i.e., making no contribution to the bonding. These calculations gave $\mu_{\text{el}} = 3.873$ D and $R_c = 1.926$ Å, both of which are considerably higher than the experimental values. Wu et al.¹⁹ calculated the properties of the lanthanide oxides using Density Functional Theory, implementing the B3LYP hybrid functionals, and found

$\mu_{el} = 4.417$ D, much higher than the observed value, and $R_e = 1.806$ Å, which is lower than the experimental value.

The dipole moment, $\mu_{el} = 2.119(8)$ D, of the upper [16.5]2 state is considerably lower than that of the two low-lying states and corresponds to a reduction in the effective charge from 0.357e in the ground state to 0.239e in the excited state. The configuration of the upper state is not known and it is not obvious what configuration would have significantly more back polarization than the ground configuration. Another possibility is that the [16.5]2 state arises from Ce^+O^- rather than $Ce^{2+}O^{2-}$ resulting in a charge transfer transition to the ground state. This would result in a looser bond and a lower B value, in agreement with observation, and a lower dipole moment. High-quality ab initio calculations on the CeO excited states would be very helpful in resolving this issue.

Conclusions

Our experiments have shown that the dipole moment for the ground state of CeO follows the general trend of the lanthanide oxide dipole moments. The equality of the dipole moments of the two lowest states indicates that the value of μ_e is determined by the configuration but not by the nature of the angular momentum coupling for electronic states within the configuration. As we have previously noted for NdO,⁵ theoretical calculations have tended to overestimate the value of the lanthanide oxide dipole moments. For CeO, the only calculation that gave a value of μ_e in good agreement with our experimental value included the 4f orbitals in the valence space¹⁸ (see above). Our measurement of the dipole moment therefore reinforces the contention¹⁸ that the 4f orbitals contribute to the bonding in the molecule.

In a future publication²⁰ we describe the determination and interpretation of electric and magnetic dipole moments of PrO. This now gives us a complete picture of the trend in electric dipole moments of the lanthanide oxides, showing that the distribution of μ_e with lanthanide nuclear mass has a slight minimum at PrO.

Acknowledgment. This work has been supported by grants from the fundamental Interactions Branch, Division of Chemical

Sciences, Department of Energy (Grant No. DE-FG02-01ER15153-A003) and by the Natural Sciences and Engineering Research Council of Canada.

Supporting Information Available: Table 1 containing the observed and observed – calculated Stark shifts in the [16.5]2–X₁2 transition and Table 2 containing the same information for the [16.5]2–X₂3 transition. This material is available free of charge via the Internet at <http://pubs.acs.org>.

References and Notes

- (1) Linton, C.; Dulick, M.; Field, R. W.; Carette, P.; Leyland, P. C.; Barrow, R. F. *J. Mol. Spectrosc.* **1983**, *102*, 441.
- (2) Dulick, M.; Field, R. W. *J. Mol. Spectrosc.* **1985**, *113*, 105.
- (3) Guo, B.; Linton, C. *J. Mol. Spectrosc.* **1991**, *147*, 120.
- (4) Chen, J.; Steimle, T. C.; Linton, C. *J. Mol. Spectrosc.* **2005**, *232*, 105.
- (5) Linton, C.; Ma, T.; Wang, H.; Steimle, T. C. *J. Chem. Phys.* **2008**, *129*, 124310.
- (6) Steimle, T. C.; Goodridge, D. M.; Linton, C. *J. Chem. Phys.* **1997**, *107*, 3723.
- (7) Linton, C.; James, A. M.; Simard, B. *J. Chem. Phys.* **1993**, *99*, 9420.
- (8) Linton, C.; Simard, B. *J. Chem. Phys.* **1992**, *96*, 1698.
- (9) Suenram, R. F.; Lovas, F. J.; Fraser, G. T.; Matsumura, K. *J. Chem. Phys.* **1990**, *92*, 4724.
- (10) Heaven, M. C.; Goncharov, V.; Steimle, T. C.; Ma, T.; Linton, C. *J. Chem. Phys.* **2006**, *125*, 204314.
- (11) Barrow, R. F.; Clements, R. M.; Harris, S. M.; Jenson, P. P. *Astrophys. J.* **1979**, *229*, 439.
- (12) Linton, C.; Dulick, M.; Field, R. W.; Carette, P.; Barrow, R. F. *J. Chem. Phys.* **1981**, *74*, 189.
- (13) Field, R. W. *Ber. Bunsenges. Phys. Chem.* **1982**, *86*, 771.
- (14) Kaledin, L. A.; McCord, J. E.; Heaven, M. C. *J. Mol. Spectrosc.* **1993**, *158*, 40.
- (15) IODINESPEC4, *Optical Photonics*, Munich, Germany (www.top-tica.com).
- (16) Schawlow, A. L. *Rev. Mod. Phys.* **1982**, *54*, 697.
- (17) Dolg, M.; Stoll, H. *Theor. Chim. Acta* **1989**, *75*, 369.
- (18) Dolg, M.; Stoll, H.; Preuss, H. *THEOCHEM* **1991**, *231*, 243.
- (19) Wu, Z. J.; Guan, W.; Meng, J.; Su, Z. M. *J. Cluster Sci.* **2007**, *18*, 444.
- (20) Wang, H.; Linton, C.; Ma, T.; Steimle, T. C. *J. Phys. Chem. A* **2009**, in press.

JP9010873